

## Study of the Fit Method for DVCS Analysis

Gagik Gavalian, UNH (2003)

### 1 Study of the Fit Method

The main challenge in the DVCS analysis from the existing CLAS electroproduction data is the separation of a single photon and more than one photon, mostly  $\pi^0$ , events in the reaction  $ep \rightarrow epX$ . In the kinematics of the DVCS analysis CLAS resolution on missing mass is not sufficient to separate cleanly these two final states. For the separation of the  $ep\gamma$  and  $ep\gamma\gamma(\pi^0)$  final states a fit to the line shape of the missing mass squared ( $MM^2$ ) distribution is used. In the kinematical range of interest three types of processes contribute to the missing system "X": 1) production of a real photon; 2)  $\pi^0$  production, and 3) the radiative processes like  $ep\gamma_R\gamma$  or  $ep\gamma_R\pi^0$ , where  $\gamma_R$  is the photon radiated by the incoming or outgoing electron. A sum of two Gaussian and a polynomial function was used in the fit, see Eq.(1). It was assumed that the missing mass distributions corresponding to the single photon and the  $\pi^0$  have a Gaussian shape, and the radiative background has a smooth polynomial shape. The difficulty in this separation method is not the fit itself, but the fact that peaks of the missing mass squared distributions for the missing photon and  $\pi^0$  events are separated by approximately one standard deviation, and therefore any small systematic uncertainties in the CLAS resolution will directly effect the fit results. (This implies, that good momentum corrections are essential for such analysis).

$$F = N_\gamma \cdot G_\gamma + N_{\pi^0} \cdot G_{\pi^0} + P \cdot Pol_2 \quad (1)$$

Here In this report we present studies performed to investigate the validity of the fit method. Studies were performed using simulated and the real data, by mixing events from a single photon and  $\pi^0$  production.

## 1.1 Studies With Experimental Data

Use of the experimental data has two advantages: i) the missing mass distributions have real physical backgrounds; ii) kinematics of selected events is the same as for the real analysis. As was mentioned above the goal is to mix identified single  $\pi^0$  and single photon events, and then reconstruct a number of each final state in the mixed sample by a fit to the missing mass distribution.

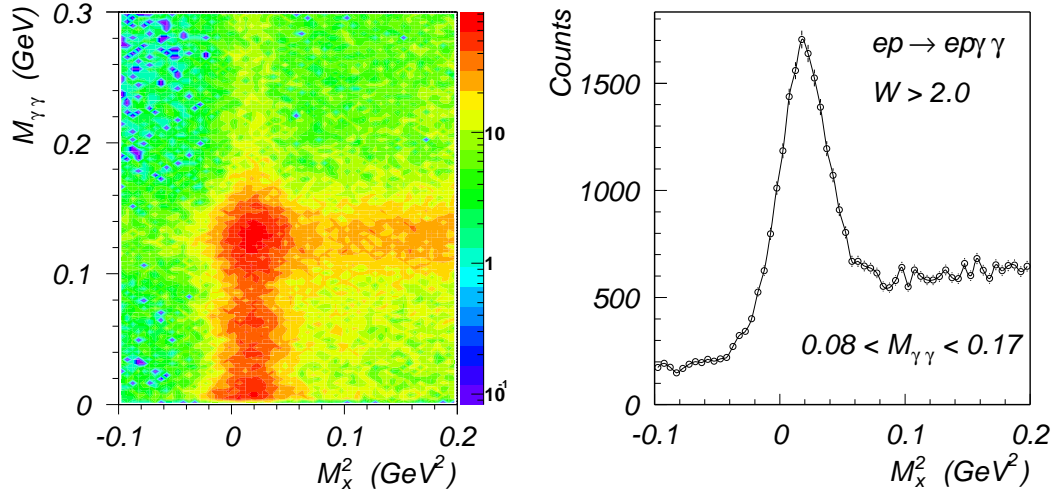


Figure 1: Selection for  $\pi^0$  events. (a)  $2\gamma$  invariant mass versus  $e'p$  missing mass (b)  $e'p$  missing mass after cut on  $2\gamma$  invariant mass.

To select  $\pi^0$  events from the experimental data final state  $ep\gamma\gamma$  is studied. A cut on the invariant mass of  $2\gamma$ s was used to select  $\pi^0$ s. In Figure 1 the invariant mass of the two photons is plotted against  $MM^2$  of the ( $e'p$ ) in the reaction  $ep \rightarrow ep\gamma\gamma X$ . A large concentration of events around  $M_{\gamma\gamma} \simeq 0.135$  GeV and the  $MM^2 \simeq 0.02$  GeV corresponds to  $\pi^0$ s.

For a single photon final state, a radiative elastic events are used in the reaction  $ep \rightarrow epX$ , when incident electron radiates a photon before the scattering. A cut on the missing momentum to be along the beam direction,  $(\Delta p_X^x/p)^2 + (\Delta p_X^y/p)^2 < 0.1$ , and a cut on the  $e'p$  scattering plane,  $178 < |\phi_e - \phi_p| < 182$ , are used to select events in this final state, see Figure 2.

Figure 3 shows the missing mass squared distributions of ( $e'p$ ) for each identified final state. Events are selected in the  $Q^2$  range from  $1.4$  GeV<sup>2</sup> to

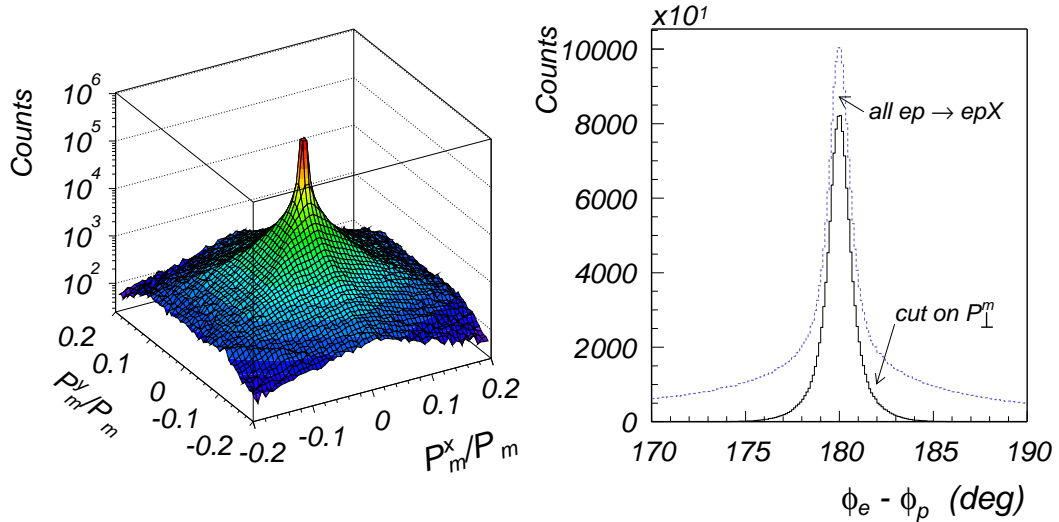


Figure 2: Radiative elastic event selection, (a) missing momentum of  $etp$ , (b) the  $etp$  scattering plane before *dashed line* and after *solid line* cuts on missing momentum.

1.9  $GeV^2$ . Fit to the spectra in Figure 3 are performed with function:

$$F = N_p G(m_p, \sigma_p) + Pol_2 \quad (2)$$

where  $N_p$  is the number of events and the  $G(m_p, \sigma_p)$  is a Gaussian function representing the  $MM^2$  distribution of the given final state, with mean  $m_p$  and standard deviation  $\sigma_p$ . In these spectra the number of a single photon events is  $N_\gamma = 946$ , and the number of the  $\pi^0$ s is  $N_{\pi^0} = 637$ .

The  $ep\gamma$  and  $ep\pi^0$  samples were mixed with different ratios. The resulting mixed distributions are fitted with function presented in Eq.1.

The mean and the  $\sigma$  of  $G_\gamma$  and  $G_{\pi^0}$  were taken from fits to the distributions in Figure 3. The shape of the background function,  $Pol_2$ , was determined by a fit to the end points of the missing mass distribution of the mixed spectrum, Figure 4,a. Figure 4,b shows the final fit to the missing mass distribution. The blue line on the graph corresponds to the background shape, the red line is the fitted Gaussian function for the photon events, and the green is the Gaussian for the  $\pi^0$  events. In the final fit the fit parameters are the number of  $ep\gamma$  ( $N_\gamma$ ) and  $ep\pi^0$  ( $N_{\pi^0}$ ) events, and the magnitude of the background ( $P$ ).

Figure 4 shows a sample of one particular mixing ratio of the  $ep\gamma$  and the  $ep\pi^0$  events. Tests were performed to check how does the fit method works

for the different ratios of initial  $ep\gamma$  and  $ep\pi^0$  events, and for the different total statistics.

Two cases were considered. In the first case the mixing ratio of the  $ep\gamma$  and  $ep\pi^0$  events was kept constant, while the total number of events in the mixed distributions were changed. The ratio of the number of thrown events (number of events from the fit to the distributions of the identified final states) to the number of reconstructed events (from the fit to the mixed distributions) was studied for different statistics. Figure 5.a shows this ratio for the different statistics (increasing from left to right). The ratio of two final states is  $\sim 1.5$ . Numbers under the each point in the plot show the number of  $ep\gamma$  events reconstructed from the fit to the radiative elastic events (the number of thrown  $ep\gamma$  events).

In the second case the number of  $ep\pi^0$  events was kept constant in the mixed distribution, while the number of  $ep\gamma$  events were gradually increased. Figure 5.b shows the ratio the thrown and the reconstructed events (described above) for the increasing  $ep\gamma$  statistics. The number of  $ep\pi^0$  events during the mixing (reconstructed from the fit to the identified  $\pi^0$  final states) is 360. Numbers under the each point show the ratio of the  $ep\gamma$  to  $ep\pi^0$  events.

In the following tables the results of fits to the different mixture of  $ep\gamma$  and  $ep\pi^0$  events, and the result of the fit to the data with constant ratio of

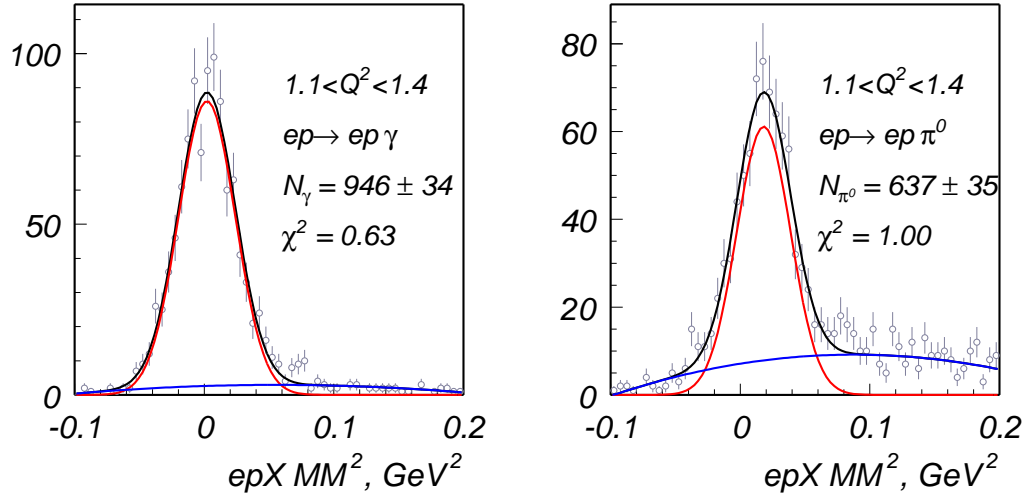


Figure 3: Fits to identified  $ep\gamma$  (a) and  $ep\pi^0$  (b) final states to determine the mean and sigmas for  $G_\gamma$  and  $G_{\pi^0}$ .

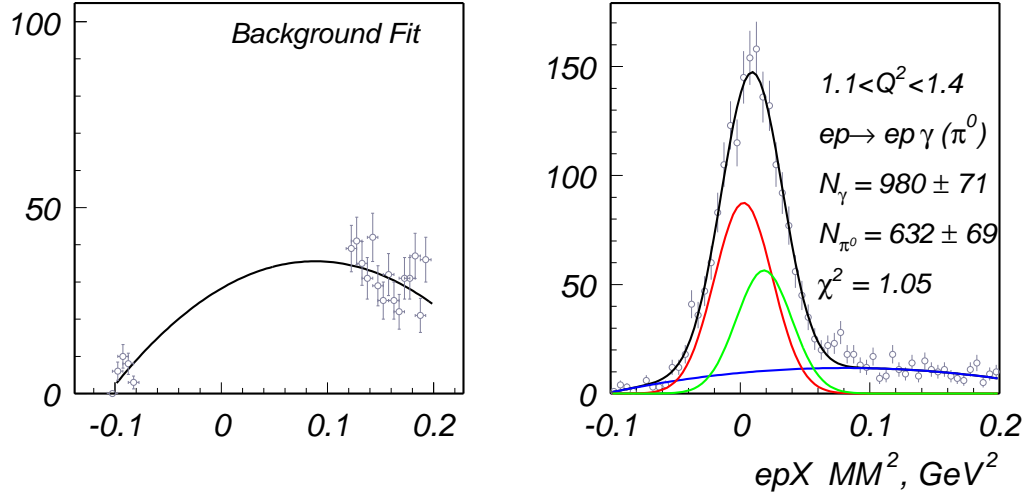


Figure 4: (a) fit to the end points of missing mass distribution for background extraction (b) Fit to missing mass with two Gaussian functions plus background to extract number of  $\gamma$ 's and  $\pi^0$  under missing mass peak.

$N_\gamma/N_{\pi^0}$  are presented.

Table 1: Results of the fit to the mixed distributions with constant mixing ratio.

N	$N_\gamma/N_{\pi^0}$	$N_\gamma^{rec}/N_\gamma^{thr}$	ERR $N_\gamma^{rec}/N_\gamma^{thr}$	$N_{\pi^0}^{rec}/N_{\pi^0}^{thr}$	ERR $N_{\pi^0}^{rec}/N_{\pi^0}^{thr}$	$N_\gamma$
1	1.49162	0.936842	0.1627500	0.868932	0.2212930	267
2	1.48780	0.961471	0.1081510	1.010960	0.1650510	550
3	1.49901	0.969152	0.0908164	1.008020	0.1360180	754
4	1.49375	0.971545	0.0804433	1.040650	0.1248140	950
5	1.51755	0.963336	0.0667195	0.998869	0.1032390	1340
6	1.50750	0.968803	0.0599815	1.030000	0.0937543	1700
7	1.51248	0.986590	0.0554076	0.988389	0.0836257	2060

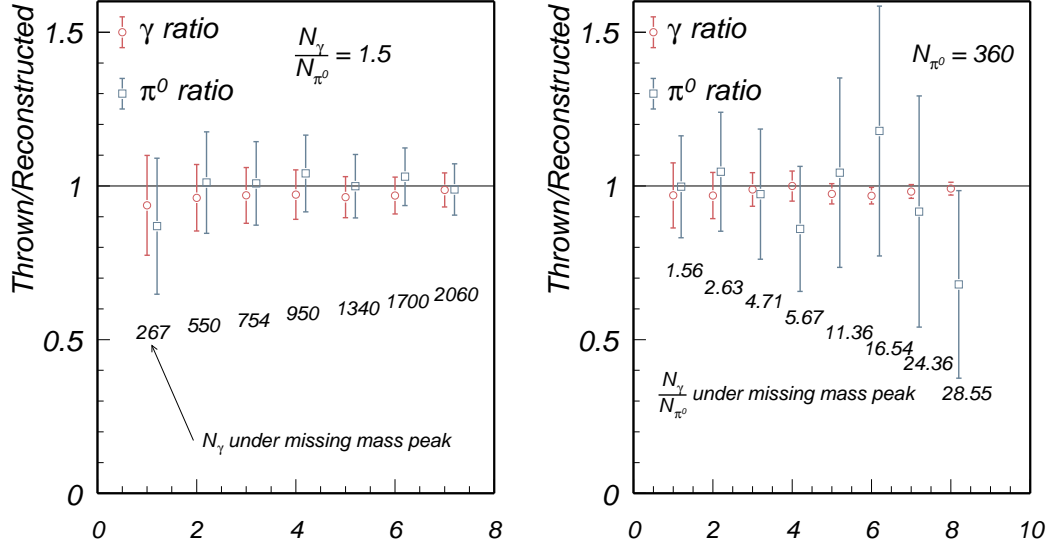


Figure 5: Ratios of reconstructed to thrown events for single photon and pion events, a) for constant  $N_\gamma/N_{\pi^0}$  ratio, b) for constant number of events in the mixed distribution.

Table 2: Results of the fit to the mixed distributions with constant number of  $\pi^0$ s.

N	$N_\gamma/N_{\pi^0}$	$N_\gamma^{rec}/N_\gamma^{thr}$	ERR $N_\gamma^{rec}/N_\gamma^{thr}$	$N_{\pi^0}^{rec}/N_{\pi^0}^{thr}$	ERR $N_{\pi^0}^{rec}/N_{\pi^0}^{thr}$	$N_{\pi^0}$
1	1.55647	0.969125	0.1057530	0.99725	0.165954	360
2	2.63361	0.968592	0.0748458	1.04611	0.193538	360
3	4.70523	0.988426	0.0542770	0.97319	0.211876	360
4	5.67493	0.999515	0.0491143	0.86019	0.203643	360
5	11.3609	0.974250	0.0331670	1.04310	0.307968	360
6	16.5372	0.968226	0.0271516	1.17857	0.406218	360
7	24.3636	0.981685	0.0224824	0.91666	0.376115	360
8	28.5455	0.991294	0.0207883	0.67977	0.305086	360

## 1.2 Tests With GSIM

Another set of tests were performed using GEANT simulated data. Events were generated using DVCS event generator (available at CLASCVS *packages/generators/dvcs*).

$ep \rightarrow ep\gamma$  and  $ep \rightarrow ep\pi^0$  final states were generated in the kinematic region which is compatible with the one in the experiment (Figure 5). Then data are processed with GEANT simulator (GSIM) and reconstructed using RECSIS (CLAS event reconstruction program).

The  $ep \rightarrow epX$  events from the both samples were mixed together and then fit procedure was performed (with function in Eq.1) to extract number of  $ep \rightarrow ep\gamma$  and  $ep \rightarrow ep\pi^0$  events. The Gaussian parameters for the fits were derived from the fit to  $ep \rightarrow ep\pi^0$  and  $ep \rightarrow ep\gamma$  events.

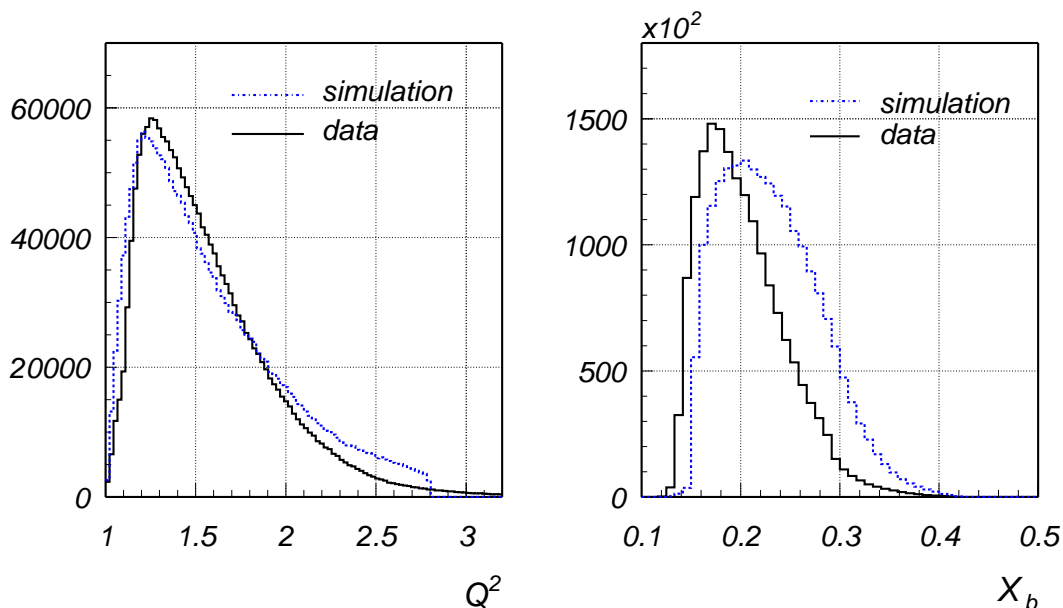


Figure 6: Simulated data kinematics compared with data.

Examples of fits for one  $\phi_{qp}$  bin are shown on Figure 8. The red dots represent thrown distribution for single gamma events, and the red line is the result of the fit to the missing mass distribution. The green circles are the single pion distribution and the green line is the result of the fit. The black points represent mixed distributions. Fit to these points are performed with function presented in Eq.(2).

Final results of fits for all  $\phi_{qp}$  bins are presented in Figure 9. Figure 9a shows the ratio of number of  $ep \rightarrow ep\gamma$  events reconstructed before mixing to the number of  $ep \rightarrow ep\gamma$  events reconstructed by the fit to the mixed distribution. The squares and circles represent the ratios for different helic-

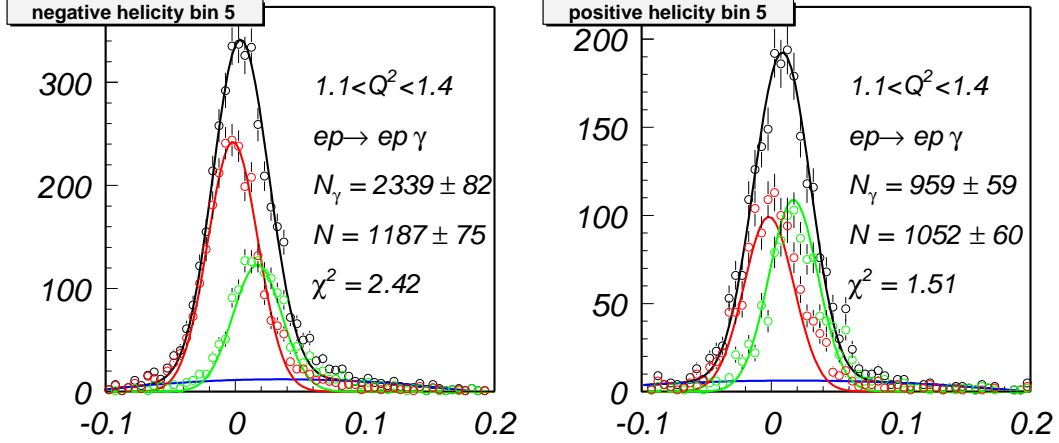


Figure 7: Missing mass squared distribution for negative (left) and positive (right) helicities fitted with two gaussians plus background for on  $\phi_{qp}, Q^2$  bin. The black points represent mixed distribution and the fit to it.

ities. The blue triangles show the ratio of ratios for negative and positive helicities. As one can see from the plot the ratio of RECSIS reconstructed events to the number of events reconstructed by fit is always bigger than one, this is due to the fact that some of the events form a background in missing mass distribution and get fitted as a part of the background. The important information is contained in triangles which show that for each  $\phi_{qp}$  bin the ratio of thrown to reconstructed events is the same for both helicities. Close to  $\phi_{qp} \sim 0^0$  due to the statistics fits do not perform as good as in other bins, but this bins do not play any significant role in the fitting.

Figure 8b shows the same results for  $ep \rightarrow ep\pi^0$  events.

After determining the number of DVCS events in each bean for both helicities the asymmetry was calculated for each  $\phi_{qp}$  bin. Extracted asymmetry as a function of  $\phi_{qp}$  is shown in Figure 10. Fit to the points is performed using function  $A = \alpha \sin\phi + \beta \sin 2\phi$ . Dotted curves on the Figure 10 represent the fit to the point from the simulated data. The number of single photon and pion events where calculated for each  $\phi_{qp}$  bin. Solid curves are the fit to the points extracted by fitting method described above.



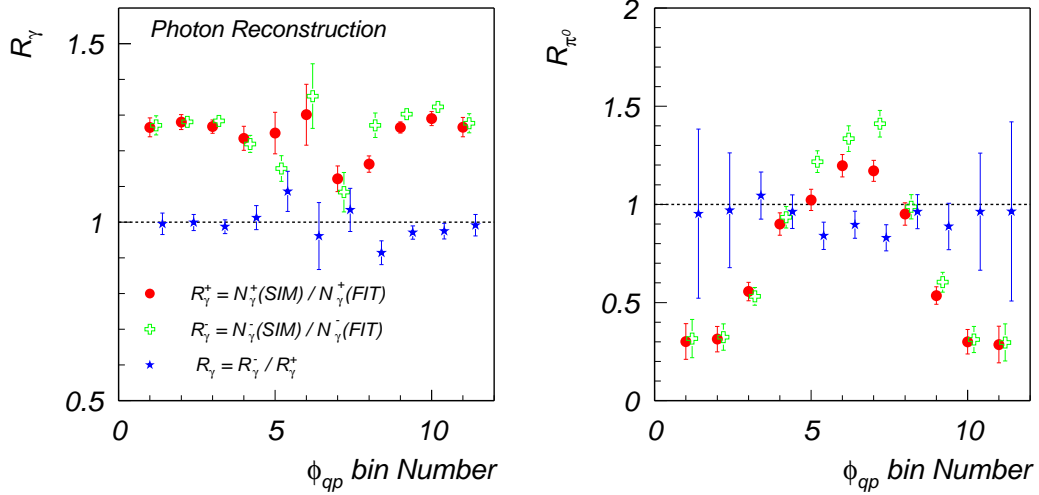


Figure 8: Fit reconstruction a) the number of reconstructed fit fit  $ep\gamma$  events divided to the number of  $ep\gamma$  events under the missing mass peak, b) the number of reconstructed fit fit  $ep\pi^0$  events divided to the number of  $ep\pi^0$  events under the missing mass peak.

## 2 Conclusions

Overall, the test show consistency of obtained results. The test performed with extracting asymmetries by using cut on missing mass square distribution show reasonable agreement with obtained result. Test preformed with data show presistency of reconstruction of number of single photon production states from mixed in different proportions data, with systematic shift below 5%. Tests with simulation show some systematic shifts of  $\sim 5\%$  in reconstructing the number of photons under missing mass square peak. Although, this systematic shifts appear to be the same for both negative and positive helicities and they do not affect the final measured asymmetry significantly. The extracted from simulated data asymmetry by using the fit method used in data shows only  $\sim 3\%$  systematical shifts.

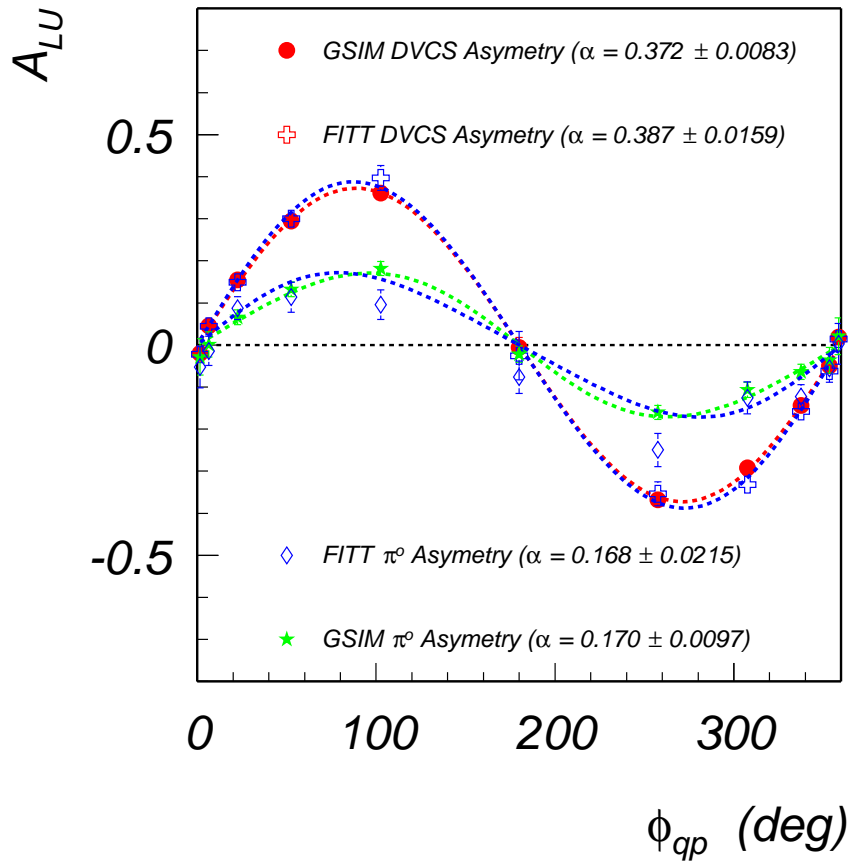


Figure 9: Extracted beam spin asymmetries for DVCS and  $\pi^0$  compared with asymmetry obtained by using missing mass fitting method. The obtained asymmetry is shifted from thrown for  $\sim 3\%$ .